JOURNAL OF MATERIALS SCIENCE 14 (1979) 663–670

# Microsegration and homogenization of Ni–7.5 wt% Al–2.0 wt% Ta dendritic monocrystals

G. D. MERZ, T. Z. KATTAMIS
*Department of Metallurgy, Institute of Materials Science, University of Connecticut, Storrs, Connecticut 06268, USA*

A. F. GIAMEI
*CDS-MERL, Pratt and Whitney Aircraft, East Hartford, Connecticut 06108, USA*

Dendritic monocrystals of nickel–7.5 wt % aluminium–2.0 wt % tantalum alloy were solidified at growth rates of 0.05 and 0.25 m $h^{-1}$, under average thermal gradients of $6 \times 10^3$ and $16 \times 10^3$ K $m^{-1}$. The segregation ratios of aluminium and tantalum were found to depend on growth conditions. That of aluminium increases only slightly with increasing local cooling rate, whereas that of tantalum increases more substantially. A diffusion model was introduced to analyse homogenization kinetics. Predictions of the index of residual segregation were in reasonable agreement with experimental measurements. Aluminium homogenizes much faster than tantalum during an isothermal treatment. It also homogenizes appreciably during crystal pulling.

In the as-cast material, the $\gamma'$ particle size is finer at locations that are poorer in aluminium and tantalum and coarser at locations that are richer in these two metals. Following a homogenization treatment, the $\gamma'$ particle size distribution becomes more uniform.

## 1. Introduction

Dendritic monocrystals of nickel-base alloys grown at high rates are both economically attractive and mechanically superior to dendritic polycrystalline material [1]. By analogy to previous findings which emphasize the beneficial effect of chemical homogeneity on mechanical properties of various alloys [2, 4], a fine cast microstructure and a uniform distribution of alloying elements within the $\gamma$-phase are highly desirable. The objective of the work reported herein was two-fold: (1) to establish the concentration variation of aluminium and tantalum across the dendritic structure of nickel–7.5 wt % aluminium–2.0 wt % tantalum and its dependence on growth conditions; (2) to study the homogenization kinetics of these two alloying elements and their dependence on cast microstructure. The unidirectional solidification of the alloy in the form of dendritic monocrystals [5], followed by quenching of the remaining liquid at a given moment, appeared most suitable for the proposed study, because of the simple geometry of the resulting dendritic structure.

## 2. Experimental procedure

Dendritic monocrystals of nickel–5.7 wt % aluminium–2.0 wt % tantalum were unidirectionally solidified under argon in an induction furnace equipped with a bottom water-cooled chill and a graphite susceptor minimizing induction stirring of the melt. The alloy was placed in an alumina crucible (0.005 m i.d. x 1.00 m long) which was lowered out of the furnace at a uniform rate of 0.05 or 0.25 m $h^{-1}$. For this particular set-up, the growth rate of the solid in the direction of heat flow, $R$, was equal to the rate at which the crucible was pulled. Two average thermal gradients in the solid–liquid region were used: $G \approx 6 \times 10^3$ K $m^{-1}$

and $G \approx 16 \times 10^3$ K m$^{-1}$. Under these growth conditions, solidification was dendritic. Growth of the dendritic monocrystal was interrupted at a given moment by quenching the remaining liquid, achieved by pulling the crucible out of the furnace at very high speed.

The temperature at a given location within the dendritic monocrystal at the moment of quench was determined by the procedure described elsewhere [5].

Specimens were taken from various locations within the dendritic monocrystals and were homogenized at 1588 K in a vacuum furnace for 2, 5 and 10 h. The distribution of aluminium and tantalum in as-solidified and in homogenized specimens was established by electron microprobe analysis, using the point counting technique. Measurements were made along various paths on two perpendicular faces of each specimen, which corresponded to longitudinal and transverse sections of the monocrystals, following a procedure described previously for unidirectionally solidified AISI 4340 low alloy steel [6]. These paths included points situated along the primary axes of dendrites, where solute concentration, $C_m$, was minimum and points situated in the interdendritic spaces, where solute concentration, $C_M$, was maximum.

## 3. Solute microsegregation

Results of microsegregation measurements, carried out on transverse sections at locations where the temperature was 1625 K at the moment of quenching, are summarized in Table I versus growth conditions. The table gives in each case $C_M$, $C_m$, as well as the corresponding segregation ratio $S = C_M/C_m$ for both aluminium and tantalum. The cooling rate at a given location, $\epsilon$, which is approximately equal to $G.R$, increases from the upper left section of the table, to the upper right, to the lower left and, finally, to the lower right section. The variation of microsegregation of aluminium in this same direction follows a regular pattern. Thus, $C_M$ and $S$ increase, whereas $C_m$ decreases with increasing local cooling rate, presumably because less time is available for back-diffusion in the dendritic solid during solidification [7]. The variation of microsegregation of tantalum follows approximately the same trend, though less regularly.

## 4. Homogenization kinetics

The "index of residual segregation", $\delta_i$, for a solute, $i$, has been previously [6] defined as:

$$\delta_i = \frac{C_M^\theta - C_m^\theta}{C_M^0 - C_m^0} \quad (1)$$

where, $C_M^\theta$ and $C_m^\theta$ are the maximum and minimum solute concentrations measured after a time, $\theta$, of homogenization. A dendrite model analogous to that used elsewhere [6] was used for calculating $\delta_i$. Detailed electron microprobe analysis was conducted on a transverse section of a dendritic monocrystal grown at 0.25 m h$^{-1}$ under a thermal gradient of $16 \times 10^3$ K m$^{-1}$ (Fig. 1). This section corresponded to a temperature of 1625 K at the moment of quenching. Isoconcentration curves for aluminium and tantalum were established and are represented in Fig. 2 for the first quadrant of the dendritic cross.

The diffusion model employed herein assumes that: (1) concentration variations along the $z$-axis (growth axis) are negligible, (2) there is complete symmetry: dendrites are columnar and symmetrically placed as shown in Fig. 3. Each dendrite can then be inscribed into a prism of approximately square cross-section, whose central axis is the locus

TABLE I Microsegregation, measured at locations corresponding to 1625 K at the moment of quench, versus growth conditions

| $R$ (m h$^{-1}$) | | $G$ (K m$^{-1}$) $6 \times 10^3$ | | | $16 \times 10^3$ | | |
|---|---|---|---|---|---|---|---|
| 0.05 | Al | $C_M = 8.05$<br>$C_m = 7.13$ | $S = 1.13$ | Al | $C_M = 8.27$<br>$C_m = 7.01$ | $S = 1.18$ |
| | Ta | $C_M = 3.28$<br>$C_m = 1.95$ | $S = 1.68$ | Ta | $C_M = 3.78$<br>$C_m = 2.05$ | $S = 1.84$ |
| 0.25 | Al | $C_M = 8.28$<br>$C_m = 6.90$ | $S = 1.20$ | Al | $C_M = 8.35$<br>$C_m = 6.75$ | $S = 1.23$ |
| | Ta | $C_M = 3.76$<br>$C_m = 2.07$ | $S = 1.82$ | Ta | $C_M = 4.10$<br>$C_m = 1.95$ | $S = 2.10$ |

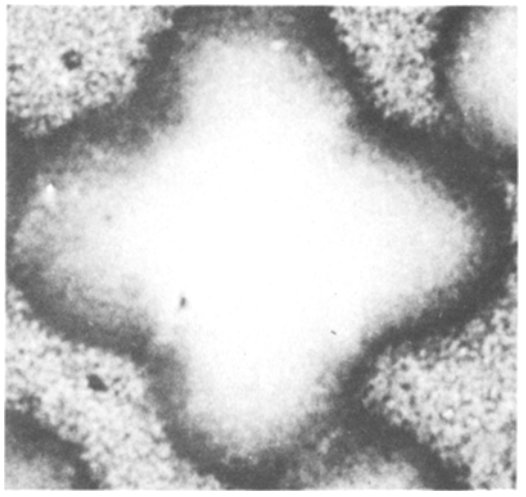

*Figure 1* Photomicrographs of a transverse section of a dendritic monocrystal of Ni–7.5 wt% Al–2.0 wt% Ta grown at 0.25 m $h^{-1}$ under a gradient of $16 \times 10^3$ K $m^{-1}$ (× 390). This section corresponded to a temperature of 1625 K at the moment of quenching.

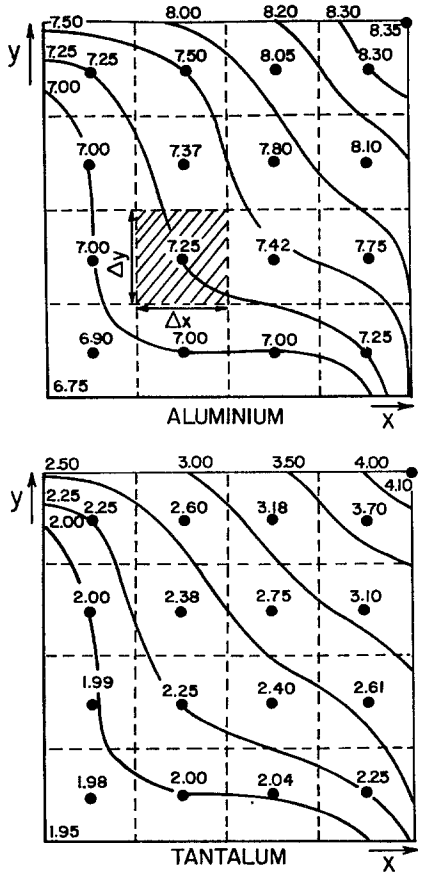


*Figure 2* Isoconcentration curves for aluminium and tantalum within a quadrant of the dendritic cross. Arm length, $l = 6.4 \times 10^{-5}$ m.

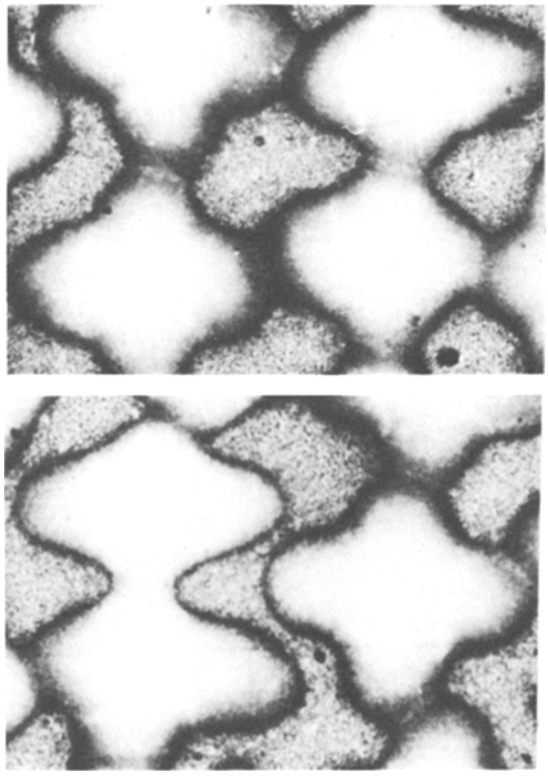

*Figure 3* Typical arrangements of primary dendrite arms in a transverse section (× 100). Ni–7.5 wt% Al–2.0 wt% Ta dendritic monocrystal.

of minimum solute concentration, $C_m$, and whose four edges are lines of maximum solute concentration, $C_M$. The solution remains valid if the prism is limited by four cylindrical isoconcentration surfaces of known, maximum solute concentration and not by four vertical edges, (3) there is no mass transfer along the growth direction; isoconcentration surfaces are, therefore, ideally cylindrical and diffusion paths are horizontal (perpendicular to the growth direction) and normal to the family of isopotential surfaces.

For diffusion in the $(x, y)$ plane (Fig. 2), the applicable differential equations are:

$$\frac{\partial C_{Al}}{\partial \theta} = D_{Al-Al}\left(\frac{\partial^2 C_{Al}}{\partial x^2} + \frac{\partial^2 C_{Al}}{\partial y^2}\right) + D_{Al-Ta}\left(\frac{\partial^2 C_{Ta}}{\partial x^2} + \frac{\partial^2 C_{Ta}}{\partial y^2}\right)$$

$$\frac{\partial C_{Ta}}{\partial \theta} = D_{Ta-Al}\left(\frac{\partial^2 C_{Al}}{\partial x^2} + \frac{\partial^2 C_{Al}}{\partial y^2}\right) + D_{Ta-Ta}\left(\frac{\partial^2 C_{Ta}}{\partial x^2} + \frac{\partial^2 C_{Ta}}{\partial y^2}\right), \quad (2)$$

where $C_{Al}$, $C_{Ta}$ are solute concentrations (wt%), $x, y$, are dimensional co-ordinates (m), $D_{Al-Al}$, $D_{Ta-Ta}$ are the on-diagonal diffusion coefficients in the solid and $D_{Al-Ta}$, $D_{Ta-Al}$ the off-diagonal coefficients ($m^2\,sec^{-1}$) and $\theta$ is time (sec). The complete absence of information on the values of $D_{Al-Ta}$ and $D_{Ta-Al}$ leads necessarily to simplification of Equation 2:

$$\frac{\partial C_{Al}}{\partial \theta} = D_{Al}\left(\frac{\partial^2 C_{Al}}{\partial x^2} + \frac{\partial^2 C_{Al}}{\partial y^2}\right)$$

$$\frac{\partial C_{Ta}}{\partial \theta} = D_{Ta}\left(\frac{\partial^2 C_{Ta}}{\partial x^2} + \frac{\partial^2 C_{Ta}}{\partial y^2}\right). \qquad (3)$$

The solution to these equations, using the same boundary conditions as previously [6] and assuming that the lengths ($l$) of the two secondary arms of the dendritic "cross" are equal (Fig. 3) can be written as

$$C_i(x,y,\theta) = \sum_{n=0}^{\infty}\sum_{n=0}^{\infty} K_{nm}\cos\left(\frac{n\pi x}{l}\right)\cos\left(\frac{m\pi y}{l}\right) \exp\left[-(n^2+m^2)\frac{\pi^2}{l^2}D_i\theta\right] + \bar{C}_i \qquad (4)$$

where $C_i(x,y,\theta)$ is the solute concentration at the point $(x,y)$ and at time $\theta$, $i$ is Al or Ta, $l$ is length of arms of the dendrite "cross", $D_i$ is the diffusion coefficient of Al or Ta in the solid Ni–Al–Ta alloy and $\bar{C}_i$ is average solute concentration.

For $n \neq 0, m \neq 0$,

$$K_{nm} = \frac{4}{l^2}\int_0^l\int_0^l f_i(x,y)\cos\frac{n\pi x}{l}\cos\frac{m\pi y}{l}\,dx dy. \qquad (5)$$

For $n = 0, m = 0$

$$K_{nm} = \frac{1}{l^2}\int_0^l\int_0^l \ldots dx dy.$$

For $n = 0, m \neq 0$, or $n \neq 0, m = 0$

$$K_{nm} = \frac{2}{l^2}\int_0^l\int_0^l \ldots dx dy$$

where,

$$f_i(x,y) = C_i^0(x,y) - \bar{C}_i$$

$C_i^0(x,y)$ = initial solute concentration of Al and Ta at the point $(x,y)$

$$C_i = \frac{1}{l^2}\int_0^l\int_0^l C_i^0(x,y)\,dx dy. \qquad (6)$$

Integrals are replaced by summations. The index of residual segregation, $\delta_i$, is finally calculated from Equation 1 after appropriate values for $C_M$ and $C_m$ have been determined from Equation 4. Details of application of this procedure for establishing the homogenization kinetics, expressed as the time variation of $\delta_i$, are given in the Appendix. Fig. 4 illustrates the variation of $\delta_{Al}$ and $\delta_{Ta}$ with $(\theta/l^2)$, as given by Equations 13 and 14. The experimental points reported on the same graph correspond to specimens grown at $1.38 \times 10^{-5}\,m\,sec^{-1}$ ($0.05\,m\,h^{-1}$) or $6.94 \times 10^{-5}\,m\,sec^{-1}$ ($0.25\,m\,h^{-1}$), under gradients of $6 \times 10^3$ or $16 \times 10^3\,K\,m^{-1}$ and homogenized for 2, 5 and 10 h. The agreement between experimental points and theoretical curves is very satisfactory, considering (a) the possible inaccuracy of adopted diffusion coefficient values, and (b) the geometric variation of isoconcentration curves with growth conditions and with location within a given dendritic monocrystal, as will be explained below. Fig. 4 emphasizes the importance of the dendrite cross arm length, $l$, in homogenization kinetics. This length is approximately equal to half the primary dendrite arm spacing or to half the primary dendrite arm spacing, times $1/\sqrt{2}$ (Fig. 3). For an ingot solidified at $1.38 \times 10^{-5}\,m\,sec^{-1}$ under a gradient of $16 \times 10^3\,K\,m^{-1}$, $l = 8.9 \times 10^{-5}$ m. After a homogenization treatment at 1588 K for 1 h, a length of time which is industrially acceptable, the residual indices of segregation for aluminium and tantalum are $\delta_{Al} = 0.3$ and $\delta_{Ta} = 0.9$. Tantalum continues

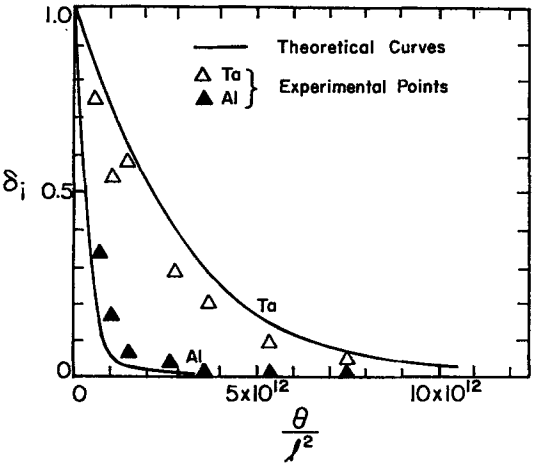


*Figure 4* Index of residual segregation, $\delta_i$, versus $\theta/l^2$ for aluminium and tantalum. Ni–7.5 wt% Al–2.0 wt% Ta dendritic monocrystals.

to be substantially segregated. Assume now that the ingot was solidified under the same gradient of $16 \times 10^3\ \mathrm{K\,m^{-1}}$ at $1.38 \times 10^{-3}\ \mathrm{m\,sec^{-1}}$, a high speed which can be achieved in a furnace equipped with a liquid tin-chill. In this case, $l = 5.5 \times 10^{-5}$ m and for a similar homogenization treatment $\delta_{Al} = 0.04$ and $\delta_{Ta} = 0.69$. The distribution of aluminium is completely uniform. Tantalum is still segregated but significantly less than in the previous case.

## 5. Homogenization during crystal pulling

The distribution of tantalum and aluminium in the solid at the completion of solidification, hence at a location where the temperature is just below the eutectic temperature, is gradually modified while the dendritic monocrystal is being pulled out of the furnace. This modification is caused by diffusion in the solid which takes place between the time at which the temperature at a given point is just below the eutectic, for example 1655 K and the time at which the temperature at that point has fallen to 1100 K. Below 1100 K the diffusion rate becomes insignificant.

Following the procedure described in the Appendix the calculation of the index of residual segregation for aluminium and tantalum, during an isothermal homogenization treatment, in a specimen taken from a location whose temperature was 1655 K at the time of quenching, yielded:

$$\delta_{Ta} = 1.014 \exp\left(-\pi^2 \frac{D\theta}{l^2}\right) - 0.014 \exp\left(-5\pi^2 \frac{D\theta}{l^2}\right) + \ldots \quad (7)$$

$$\delta_{Al} = 1.067 \exp\left(-\pi^2 \frac{D\theta}{l^2}\right) - 0.067 \exp\left(-5\pi^2 \frac{D\theta}{l^2}\right) + \ldots . \quad (8)$$

Let $C_M^i$, $C_m^i$ be the maximum and minimum solute concentrations at 1655 K and $C_M^f$, $C_m^f$ those at 1100 K. The index of residual segregation after continuous cooling from 1655 K to 1100 K can then be expressed as:

$$\delta = A \exp\left[\left(-\frac{\pi^2}{l^2}\right) \int D\mathrm{d}\theta\right] + B \exp\left[\left(-5\frac{\pi^2}{l^2}\right) \int D\mathrm{d}\theta\right] + \ldots , \quad (9)$$

where, $A$ and $B$ are constants which depend on the geometry of isoconcentration curves.

$$\int D\mathrm{d}\theta = \int \frac{D\mathrm{d}T}{(\mathrm{d}T/\mathrm{d}\theta)},$$

and replacing integrals by summations:

$$\frac{1}{\epsilon} \int D\mathrm{d}T = \frac{D_0 . \Delta T}{\epsilon} \sum_{1655}^{1100} \exp\left(-\frac{Q}{RT}\right), \quad (10)$$

where: $\epsilon = \mathrm{d}T/\mathrm{d}\theta = G.R$, cooling rate ($K\,\mathrm{sec^{-1}}$), $D_0 = 2.05 \times 10^{-4}(\mathrm{m^2\,sec^{-1}})$ for tantalum and

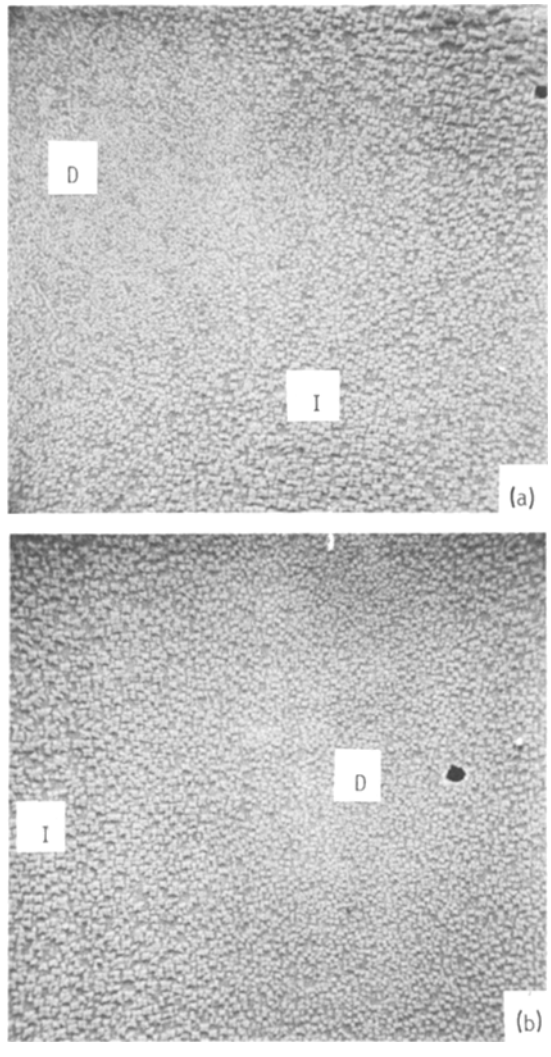


*Figure 5* Scanning electron micrographs of (a) transverse section, and (b) a longitudinal section, (× 780). Ni–7.5 wt% Al–2.0 wt% Ta dendritic monocrystal grown at $0.25\ \mathrm{m\,h^{-1}}$ under a gradient of $16 \times 10^3\ \mathrm{K\,m^{-1}}$. D = dendrite centre, I = interdendritic space.

$1.87 \times 10^{-4}$ ($m^2\,sec^{-1}$) for aluminium. $Q/R$ = 35 625 for tantalum and 32 000 for aluminium. Finally, Equations 7 and 8 become:

$$\delta_{Ta} = 1.014 \exp\left(-1.054 \times 10^{-11} \frac{\pi^2}{l^2 \epsilon}\right) - 0.014 \exp\left(-5.27 \times 10^{-11} \frac{\pi^2}{l^2 \epsilon}\right) + \ldots \quad (11)$$

and

$$\delta_{Al} = 1.067 \exp\left(-8.664 \times 10^{-11} \frac{\pi^2}{l^2 \epsilon}\right) - 0.067 \exp\left(-4.332 \times 10^{-10} \frac{\pi^2}{l^2 \epsilon}\right) + \ldots \quad (12)$$

As an example, assume that a monocrystal is solidified at $6.92 \times 10^{-5}$ m $sec^{-1}$ under a gradient of $6 \times 10^3$ K $m^{-1}$. The corresponding average cooling rate $\epsilon = 0{\cdot}416$ m $sec^{-1}$ and Equations 11 and 12 yield:

$$\delta_{Ta} = 0{\cdot}963 \quad \text{and} \quad \delta_{Al} = 0.759.$$

It is obvious that an appreciable homogenization of aluminium, the fast diffusing species, has taken place during cooling. That of tantalum is by far less significant.

## 6. γ′ precipitate

An examination of the geometry of the γ′ precipitate with scanning electron microscopy shows clearly that particle size depends on location within the dendritic structure, hence on local aluminium and tantalum concentrations. Fig. 5a and b shows that the γ′ particle size is finer in the centre of dendrites, where concentrations of aluminium and tantalum are lower and coarser in the interdendritic species, where these concentrations are higher. The same observation can be made at a higher magnification in Figs 6a and b, which also shows the existence of a second generation of fine γ′ precipitate between the coarser particles. While the coarser generation precipitated during continuous pulling of the monocrystal, the finer generation formed during quenching.

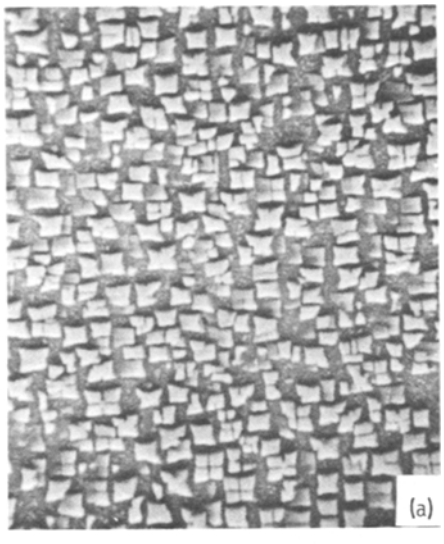



*Figure 6* Scanning electron micrographs of a longitudinal section of an Ni–7.5 wt% Al–2.0 wt% Ta dendritic monocrystal solidified at 0.25 m $h^{-1}$ under a gradient of $16 \times 10^3$ K $m^{-1}$. (a) Centre of dendrite (× 3900), (b) interdendritic region (× 3900), (c) homogenized specimen, (× 780).

The dependence of $\gamma'$ particle size on local solute concentration is analogous to that established previously for cast Inconel 713C alloy [8]. In regions which are richer in solute the solvus temperature is higher [5] and $\gamma'$ precipitation occurs earlier than in regions which are poorer in solute. Thus, coarsening of the precipitate operates for a longer time in interdendritic regions and this explains why particle size is coarser in these regions (average particle size $= 1.4 \times 10^{-6}$ m) compared with that in the centre of the dendrite (average particle size $= 0.87 \times 10^{-6}$ m). No significant variation of the vol% $\gamma'$ was found across the dendritic structure.

As illustrated in Fig. 6 the distributions of $\gamma'$ particles across the $\gamma$ matrix and of the $\gamma'$ particle size become more uniform after homogenization. This is understandable because after the homogenization treatment the distribution of solute, hence the solvus temperature and coarsening time are more uniform. The mechanical behaviour of precipitation-hardened alloys is known to depend on precipitate particle geometry. It can be speculated that the beneficial effect of homogenization on properties of nickel-base superalloys is, at least partly, due to the above-mentioned effect of the treatment on $\gamma'$ particle size and distribution.

## 7. Conclusions

(1) The segregation ratios of aluminium and tantalum in dendritic monocrystals of Ni–7.5 wt% Al–2.0 wt% Ta depend on growth conditions $R$ and $G$. They increase with increasing local cooling rate, $G.R$.

(2) Homogenization kinetics based on a diffusion model which assumes prismatic dendrites led to predictions of the index of residual segregation for aluminium and tantalum which are fairly close to those measured experimentally on specimens homogenized for 2, 5 and 10 h at 1588 K.

(3) A longer time is necessary for tantalum than for aluminium in order to achieve the same index of residual segregation.

(4) An appreciable homogenization of aluminium takes place during crystal pulling. That of tantalum is by far less significant.

(5) In the as-cast material the $\gamma'$ particle size is finer at locations which are poorer in aluminium and tantalum and coarser at locations which are richer in these two metals. Following a homogenization treatment the $\gamma'$ particle size distribution becomes more uniform.

## Appendix. Calculation of the index of residual segregation

### A.1. $\delta_{Al}$

The square of corners (0, 0), ($l$, 0), ($l$, $l$) and (0, $l$) was divided into sixteen partial squares (Fig. 2). The solute concentrations at any point of a square was taken equal to the concentration at the centre of that square. The average concentration of all partial squares is $\bar{C}_{Al} = 7.434$ at time 0; the $f_{Al}(x, y) = C^{\circ}_{Al} - \bar{C}_{Al}$ at the different rectangles can then be calculated. Choosing for $m$ and $n$ the values: 0, 1, 2, the following values for $K_{nm}$ were found: $K_{0,0} = 0$, $K_{0,} = -0.380$, $K_{0,2} = -0.082$, $K_{1,0} = -0.422$, $K_{1,1} = 0.237$, $K_{1,2} = 0.076$, $K_{2,0} = 0.0142$, $K_{2,1} = 0.033$ and $K_{2,2} = 0.017$.

The following expression was derived:

$$\delta_{Al} = 1.157 \exp\left(-\pi^2 \frac{D\theta}{l^2}\right) - 0.157 \exp\left(-5\pi^2 \frac{D\theta}{l^2}\right) + \ldots . \tag{13}$$

The diffusion coefficient for Al adopted here is: $D_{Al} = 1.87 \exp(-64\,000/RT)$ [9]. At the homogenization temperature of 1588 K, $D_{Al} = 3.313 \times 10^{-13}$ m$^2$ sec$^{-1}$ and Equation 13 becomes:

$$\delta_{Al} = 1.157 \exp\left[-32.69 \times 10^{-13}\left(\frac{\theta}{l^2}\right)\right] - 0.157 \exp\left[-163.48 \times 10^{-13}\left(\frac{\theta}{l^2}\right)\right] + \ldots . \tag{14}$$

### A.2. $\delta_{Ta}$

Following the same procedure as for aluminium, the average concentration of all partial squares is $\bar{C}_{Ta} = 2.467$ at time 0; the $f_{Ta}(x, y) = C^{\circ}_{Ta} - \bar{C}_{Ta}$ at the different rectangles is then calculated. The various values of $K_{nm}$ are: $K_{0,0} = 0$, $K_{0,1} = -0.468$, $K_{0,2} = 0.063$, $K_{1,0} = -0.441$, $K_{1,1} = 0.328$, $K_{1,2} = 0.00$, $K_{2,0} = 0.007$, $K_{2,1} = 0.034$ and $K_{2,2} = 0.035$. The following expression was derived for the index of residual segregation of tantalum:

$$\delta_{Ta} = 1.038 \exp\left(-\pi^2 \frac{D\theta}{l^2}\right)$$

$$-0.038 \exp\left(-5\pi^2 \frac{D\theta}{l^2}\right) + \ldots . (15)$$

The value adopted for the diffusion coefficient of Ta in the alloy [9] is:

$$D_{Ta} = 2.05 \exp\left(-\frac{71\,250}{RT}\right). \text{ At } 1588\,\text{K},$$

$$D_{Ta} = 3.70 \times 10^{-4}\,\text{m}^2\,\text{sec}^{-1}$$

and

$$\delta_{Ta} = 1.038 \exp\left[-3.65 \times 10^{-13}\left(\frac{\theta}{l^2}\right)\right]$$

$$-0.038 \exp\left[-18.258 \times 10^{-13}\left(\frac{\theta}{l^2}\right)\right] + \ldots . (16)$$


## Acknowledgement

The authors are thankful to the Air Force Office of Scientific Research for supporting this work under Grant No. 77–3344 to the University of Connecticut. Microprobe analysis was performed at Pratt and Whitney.


## References


1. B. H. KEAR and B. J. PIEARCEY, *Trans. Met. Soc. AIME* **238** (1967) 1209.
2. F. C. QUIGLEY and P. J. AHEARN, *Trans. AFS* **72** (1964) 813.
3. S. N. SINGH and M. C. FLEMINGS, *Trans. Met. Soc. AIME* **245** (1969) 1811.
4. G. D. MERZ and T. Z. KATTAMIS, *Met. Trans.* **8A** (1977) 295.
5. T. Z. KATTAMIS and J. C. LECOMTE, *J. Mater Sci.* **13** (1978) 2731.
6. T. Z. KATTAMIS and M. C. FLEMINGS, *Trans. Met. Soc. AIME* **233** (1965) 992.
7. H. D. BRODY and M. C. FLEMINGS, *ibid* **236** (1966) 615.
8. A. J. BHAMBRI and T. Z. KATTAMIS, *Met. Trans.* **6B** (1975) 523.
9. C. J. SMITHELLS, "Metals Reference Book", 5th Edn. (Butterworths, London, 1976).


Received 22 May and accepted 19 July 1979.